Korean J. Chem. Eng., **22**(1), 9-16 (2005)

Nusselt Numbers for Longitudinal Laminar Flow in Shell-and-Tube Exchangers

Sangkyun Koo and Sang-Yoon Kang*,†

Department of Chemical Engineering and Materials Science, Syracuse University, Syracuse, NY 13244, U.S.A.
*Korean Intellectual Property Office, Government Complex-Daejeon, Daejeon 302-701, Korea
(*Received 2 August 2004 • accepted 2 November 2004*)

Abstract−The problem of determining shell side Nusselt numbers for a countercurrent, shell-and-tube configuration is examined in detail for square and hexagonal arrays of tubes when the shell side flow is laminar and parallel to the tubes. A multipole expansion method is employed to determine fluid velocity and temperature field for the fluid on the shell side. The numerical results for the shell side Nusselt numbers are compared with those by a cell theory and an asymptotic analysis. The cell theory agrees well with the numerical results at small area fractions and gives better estimates for hexagonal arrays. The results for the hexagonal arrays are in agreement with those of Sparrow et al. [1961]. The asymptotic analysis shows better agreement with the numerical results for wider range of area fractions of tubes in square and hexagonal arrays. In addition, we determine shell side Nusselt number as a function of the ratio of thermal conductivities of the fluids on the tube and shell side. Finally, we present formulas for determining Nusselt numbers for the periodic arrays.

Key words: Nusselt Number, Shell-and-Tube Exchanger, Asymptotic Analysis, Cell Theory, Square and Hexagonal Arrays

INTRODUCTION

Shell and tube configurations are commonly used in heat and mass transfer equipment such as hollow fiber modules used in gas separation by membranes and heat exchangers. Because of their widespread use in industry, a number of investigators have analytically studied the problem of predicting heat or mass transfer coefficients. The overall heat (or mass) transfer coefficient is generally expressed as a sum of resistances offered by the tube and shell sides, and the transport of heat or mass is examined separately for the tube and shell sides. The problem of determining the tube side heat transfer coefficient under laminar flow conditions was first formulated by Graetz who considered the cases of constant wall temperature and constant wall heat flux separately. Analytical solutions for these problems were obtained by Papoutsakis et al. [1981]. The limiting cases such as transport at small or large axial distances have also been examined, and the results may be found in standard text books for heat and mass transfer (see, e.g., Bird, Stewart and Lightfoot [1960]). An interesting analysis for the limiting case of small Peclet number has been presented by Acrivos [1980].

For the case of shell side, a number of experimental investigations have been performed due to their practical importance in industry. Kim and Aicher [1997] empirically examined heat transfer on the shell side for various geometries of shell-and-tube heat exchangers. However, theoretical studies for the case of shell side are rare. The heat transfer coefficient for the shell side for the case when the mean flow direction is perpendicular to the tubes was determined in the limit of small Peclet and small Reynolds numbers by Sangani and Acrivos [1982] and that in the limit of small Reynolds number but large Peclet number by Wang and Sangani [1997].

The present study is concerned with the longitudinal case, i.e., the case of flow parallel to the tubes in periodic arrangements. Specifically, we determine Nusselt numbers for fully developed shell side laminar flow parallel to tubes in square and hexagonal arrays. We examine in detail a special situation in which the thermal inertia, i.e., the product of mass flow rate and heat capacity, of the shell and tube side fluids is equal. For this case, the average temperature profiles of the fluids are linear and heat transfer across the tubes is independent of the axial position. This is equivalent to the case of constant wall heat flux examined by Sparrow et al. [1961].

The common practice of separating the overall resistance to heat transfer into resistances on the tube and shell side and assuming that the Nusselt number on the tube and shell sides depends only on the Reynolds and Peclet numbers on each side is not strictly true for fully developed flows. Thus, for example, the shell side heat transfer coefficient depends additionally on the ratio of thermal conductivities of the fluids on the tube and shell side. It is shown that the dependence on the ratio is rather weak at small to modest area fractions but not so for high area fractions. The results for Nusselt numbers for square and hexagonal arrays are compared with a cell theory approximation and an asymptotic analysis for small area fractions of tubes. Agreement between the cell theory and numerical results is excellent at small area fractions. At larger area fractions, the cell theory gives better estimates for hexagonal arrays. The asymptotic analysis is shown to give more accurate results than does the cell theory for both square and hexagonal arrays.

This paper is organized as follows. The governing equations and the method are described in detail in Section 2. The theory and results are presented in Sections 3, and the conclusion of this work is given in Section 4.

FORMULATION OF THE PROBLEM AND THE METHOD

We consider a countercurrent shell and tube configuration as shown

†To whom correspondence should be addressed.
E-mail: kangsa2@nate.com

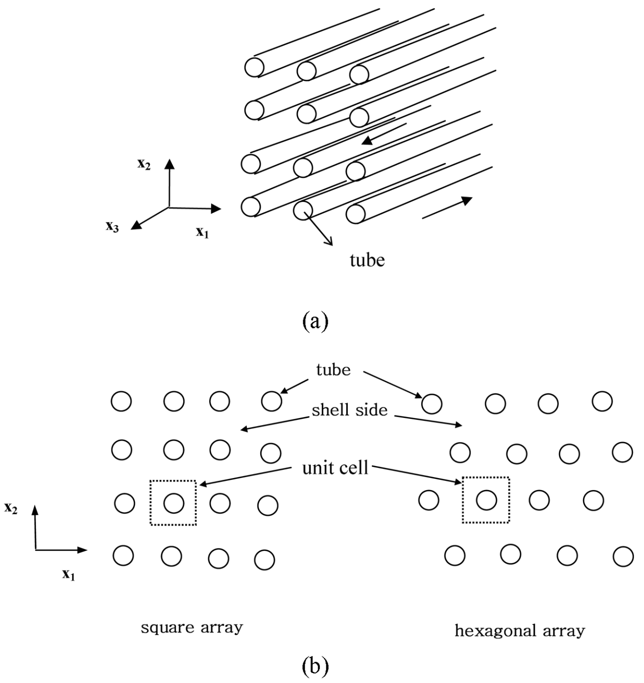

Fig. 1. (a) Schematic diagam of a shell-and-tube configuration, (b) Square and hexagonal arrays.

in Fig. 1. The flow on both sides is laminar and unidirectional. The fluids undergo no phase change, and, to simplify the analysis, we consider the case when the product of the mass flow rate and heat capacity for the fluid on the shell side equals that on the tube side. For this special case the average temperatures of the fluids on the tube and shell sides increase linearly with the axial distance. With no loss of generality, we let the average temperature gradient to equal 1/Pe and write

$$T_t^*(x_1, x_2, x_3)=(x_3/Pe)+T_t(x_1, x_2) \tag{1}$$

$$T_s^*(x_1, x_2, x_3)=(x_3/Pe)+T_s(x_1, x_2). \tag{2}$$

Here, x_3-axis is taken to be along the axes of the tubes and (x_1, x_2) are the coordinates of a point in the plane normal to the tubes. The distances are non-dimensionalized by a, the radius of the tubes. Pe= $\rho c_p Ua/k$ is the Peclet number based on flow outside the tubes. U is the superficial velocity of the fluid on the shell side, ρ, c_p and k are, respectively, the density, specific heat, and thermal conductivity of the shell side fluid. Upon substitution of (2) into energy equation for the fluid on the shell side we obtain

$$\nabla^2 T_s = u_s, \tag{3}$$

where u_s is the velocity of the fluid non-dimensionalized by the superficial velocity U, and

$$\nabla^2 = \frac{\partial^2}{\partial x_1^2} + \frac{\partial^2}{\partial x_2^2} \tag{4}$$

is the Laplacian operator in the x_1-x_2 plane. Since we have taken the product of mass flow rate and heat capacity for tube and shell side fluids to be equal, the average velocity of the fluid inside a tube equals $\rho c_p U/(\phi \rho_t c_{pt})$, where ρ_t and c_{pt} are, respectively, the density and specific heat of the tube side fluid and ϕ is the area fraction of the tubes. The energy equation for the tube side fluid reduces to

$$\nabla^2 T_t = -u_t/(\alpha_c \phi), \tag{5}$$

where $\alpha_c=k_t/k$ is the ratio of fluid thermal conductivities, and u_t is the standard non-dimensional parabolic profile for laminar flow through circular tubes. For a tube centered at origin, we have

$$u_t=2(1-r^2). \tag{6}$$

Here, r is the radial distance from the center of the tube. The negative sign on the right-hand-side of (5) accounts for the countercurrent nature of the flows on the tube and shell sides.

The positions of the center of N tubes will be denoted by $\mathbf{x}^\alpha$, α= 1, 2, ..., N. These centers lie within a unit cell that is extended periodically. Note that N is unity for square and hexagonal arrays of tubes. The boundary conditions for temperature are therefore spatial periodicity and continuity of temperature and flux at the surface of the tubes:

$$T_s = T_t, \quad \mathbf{n}\cdot\nabla T_s = \alpha_c \mathbf{n}\cdot\nabla T_t \quad \text{at } |\mathbf{x}-\mathbf{x}^\alpha| = 1. \tag{7}$$

Note that we have assumed that the tube wall thickness is negligibly small and it offers no resistance to the heat transfer.

We shall be interested in Nusselt number, the non-dimensional heat transfer coefficient. The overall Nusselt number is defined as

$$Nu_{overall} = \frac{ah_{overall}}{k} = \frac{Q}{2\pi k \Delta T_{overall}}, \tag{8}$$

where Q is the rate of heat transfer per tube per unit length of the exchanger and $\Delta T_{overall}$ is the difference between the average temperatures of the fluid on the tube and shell sides. We shall use two kinds of averages. The first is a spatial average

$$\langle T_s \rangle = \frac{1}{(1-\phi)\tau}\int_{D_s} T_s dA, \tag{9}$$

and the second is a fluid velocity weighted average, referred to in the literature as the mixing-cup temperature,

$$\langle T_s \rangle_c = \frac{1}{\tau}\int_{D_s} u_s T_s dA. \tag{10}$$

Here, τ is the area of the unit cell non-dimensionalized by a^2 and D_s is the area occupied by the shell side fluid. Note that the integral in (10) is divided by τ only since the velocity is non-dimensionalized by the superficial velocity and hence

$$\int_{D_s} u_s dA = \tau. \tag{11}$$

The average temperatures for the tube side fluid are defined in a similar manner.

The heat transfer per tube can be related to the average temperature gradient. Thus, from heat flux, (3) and (11), it is easy to show that

$$Q = \frac{k\tau}{N} = \frac{k}{\pi\phi}. \tag{12}$$

Substituting for Q in (8) we obtain

$$Nu_{overall} = \frac{1}{2\phi \Delta T_{overall}}. \tag{13}$$

We shall use the method of multipole expansion for determining the velocity and temperature fields.

The method uses periodic fundamental singular solutions of Laplace and bi-harmonic equations and their derivatives to construct velocity and temperature fields. We shall describe here in more detail the procedure for determining the velocity field which follows the analysis presented in Sangani and Yao [1988].

1. Velocity Field

The shell side fluid velocity satisfies

$$\nabla^2 u_s = G, \tag{14}$$

where G is the pressure gradient non-dimensionalized by $\mu U/a^2$. A multipole expansion expression for the velocity field is given by [Sangani and Yao, 1988]

$$u_s = U_0 + \sum_{\alpha=1}^{N}\sum_{n=0}^{\infty}[A_n^\alpha \partial_1^n + \tilde{A}_n^\alpha \partial_1^{n-1}\partial_2]S_1(\mathbf{x}-\mathbf{x}^\alpha), \tag{15}$$

where A_n^α and $\tilde{A}_n^\alpha$ are the 2^n-multipoles induced by the presence of tube α, $\tilde{A}_0 \equiv 0$, and $\partial_k^n = (\partial^n/\partial x_k^n)$ (k=1, 2) is a short-hand notation for the n-th order partial derivative with respect to x_k. The function S_1 is a spatially periodic function satisfying [Hasimoto, 1959]

$$\nabla^2 S_1(\mathbf{x}) = 4\pi\left[\frac{1}{\tau} - \sum_{x_L}\delta(\mathbf{x}-\mathbf{x}_L)\right]. \tag{16}$$

In the above expression, $\mathbf{x}_L$ are the coordinates of the lattice points of the array and δ is Dirac's delta function. In addition to the above differential equation, we require that the integral of S_1 over the unit cell be zero. A Fourier series representation of S_1 and an efficient technique based on Ewald summation for evaluating S_1 are described by Hasimoto [1959].

Substituting (15) into (14), and making use of (16), we find that the non-dimensional pressure gradient is related to the sum of monopoles:

$$G = \frac{4\pi}{\tau}\sum_{\alpha=1}^{N} A_0^\alpha = 4\phi\langle A_0\rangle, \tag{17}$$

where $\langle A_0 \rangle$ is the average monopole. The multipoles A_n^α and $\tilde{A}_n^\alpha$ and the constant U_0 in (15) are to be determined from the no-slip boundary condition u_s=0 on the surface of the tubes and (11), which states that the non-dimensional superficial velocity is unity. For this purpose it is convenient to re-expand u_s around the center of each tube. For example, u_s is expanded near tube α as

$$u_s = \sum_{n=0}^{\infty}[u_n^\alpha(r)\cos n\theta + \tilde{u}_n^\alpha(r)\sin n\theta] \tag{18}$$

with

$$u_n^\alpha(r) = a_n^\alpha r^{-n} + e_n^\alpha \quad n \ge 1, \qquad u_0^\alpha(r) = a_0^\alpha \log r + e_0^\alpha + Gr^2/4, \tag{19}$$

where $r=|\mathbf{x}-\mathbf{x}^\alpha|$. The terms singular at r=0 in the above expression arise from the singular part of S_1 at r=0. Noting that S_1 behaves as $-2\log r$ as $r\to 0$ [Hasimoto, 1959], and using the formulas for the derivatives of log r given in Appendix, we obtain

$$a_0^\alpha = -2A_0^\alpha, \qquad a_n^\alpha = 2(-1)^n(n-1)!A_n^\alpha \qquad (n \ge 1). \tag{20}$$

The coefficients $\tilde{A}_n^\alpha$ are similarly related to $\tilde{a}_n^\alpha$.

The coefficients of the regular terms, such as e_n^α, are related to the derivatives of the regular part of u_s at $\mathbf{x}=\mathbf{x}^\alpha$ [Sangani and Yao, 1988]. For example,

$$e_n^\alpha = \frac{1}{n!}[\partial_1^n - \xi_n\partial_1^{n-2}\nabla^2]u_s^r(\mathbf{x}^\alpha), \tag{21}$$

$$\tilde{e}_n^\alpha = \frac{1}{n!}[\partial_1^{n-1}\partial_2 - \tilde{\xi}_n\partial_1^{n-3}\partial_3\nabla^2]u_s^r(\mathbf{x}^\alpha), \tag{22}$$

where ξ_n=n/4 for n≥2, $\tilde{\xi}_n$=(n−2)/4 for n≥3, and $\xi_0=\xi_1=\tilde{\xi}_1=\tilde{\xi}_2=0$. In (21)-(22), u_s^r denotes the regular part u_s obtained by removing the singular part, $-2\log r$, from $S_1(\mathbf{x}-\mathbf{x}^\alpha)$.

To determine the relation between U_0 in (15) and the superficial velocity we must integrate u_s over the area D_s occupied by the shell side fluid. Since the integrals of S_1 and its derivatives over the unit cell vanish, it is easier to evaluate the integral of u_s over D_s by integrating (15) over the unit cell and subtracting from it the integral of u_s inside the tubes. With the non-dimensional superficial velocity taken as unity, the above procedure yields

$$1 = U_0 - \frac{1}{\tau}\sum_{\alpha=1}^{N}\int_{r=0}^{1}\int_{\theta=0}^{2\pi}u_s^\alpha(r,\theta)r\,dr\,d\theta. \tag{23}$$

Care must be taken in carrying out above integration to account for the singular nature of u_s^α at $\mathbf{x}=\mathbf{x}^\alpha$. Upon carrying out integration, we obtain

$$U_0 = 1 + \phi(1-\phi/2)\langle A_0\rangle + 2\phi\langle A_2\rangle. \tag{24}$$

The last term on the right-hand-side of the above equation was missing in the expression given in Sangani and Yao [1988]. Fortunately, the omission of this term led to only small numerical error in the results for pressure drop presented by these investigators.

The no-slip boundary condition on the surface of the tube, together with the orthogonality of trigonometric functions, requires that

$$u_n^\alpha(1) = \tilde{u}_n^\alpha(1) = 0. \tag{25}$$

Substituting for a_n^α and e_n^α from (20) and (21) into expressions for u_n^α and applying (25) we obtain a set of linear equations in the multipole coefficients A_n^α. This set is truncated by retaining only the terms with $n \le N_s$ to yield a total of $2N_s+1$ equations in the same number of unknowns, solving which yields the velocity of the fluid on the shell side.

2. Temperature Field

The temperature of the fluid on the shell side is determined in a similar manner. A formal solution of (3) that is spatially periodic is given by

$$\begin{aligned} T_s(x) = \sum_{\alpha=1}^{N}\sum_{n=0}^{\infty}&[B_n^\alpha\partial_1^n + \tilde{B}_n^\alpha\partial_1^{n-1}\partial_2]S_1(\mathbf{x}-\mathbf{x}^\alpha) \\ &+ [A_n^\alpha\partial_1^n + \tilde{A}_n^\alpha\partial_1^{n-1}\partial_2]S_2(\mathbf{x}-\mathbf{x}^\alpha) \end{aligned} \tag{26}$$

where the spatially periodic function S_2 satisfies

$$\nabla^2 S_2 = S_1 \tag{27}$$

As shown by Hasimoto [1959]

$$S_m(\mathbf{x}) = \frac{1}{\pi\tau(-4\pi^2)^{m-1}}\sum_{\mathbf{k}\neq\mathbf{0}}k^{-2m}\exp(2\pi i\mathbf{k}\cdot\mathbf{x}), \tag{28}$$

where the summation is over all reciprocal lattice vectors except $\mathbf{k}=\mathbf{0}$. As mentioned earlier, Hasimoto [1959] has described a method for evaluating these functions using the Ewald summation technique.

Substituting for T_s and u_s from (26) and (15) into (3) and using

(16) and (27), we find that, in order for (26) to be the solution for T_s, we must have

$$\frac{4\pi}{\tau}\sum_{\alpha=1}^{N}B_0^\alpha=U_0. \tag{29}$$

To determine the multipoles B_n, we expand T_s near the center of each tube. Near tube α

$$T_s(\mathbf{x})=\sum_{n=0}^{\infty}f_n^\alpha(r)\cos n\theta+\tilde{f}_n^\alpha(r)\sin n\theta, \tag{30}$$

with

$$f_n^\alpha=-\frac{1}{4}r^2(1-\log r)a_0^\alpha+\frac{r^2}{4}e_0^\alpha+b_0^\alpha\log r+g_0+\frac{r^4}{64}G, \tag{31}$$

$$f_1^\alpha=\frac{1}{2}r\left(\log r-\frac{1}{2}\right)a_1^\alpha+\frac{r^3}{8}e_1^\alpha+b_1^\alpha r^{-1}+g_1^\alpha r, \tag{32}$$

$$f_n^\alpha=\frac{r^{2-n}}{4(1-n)}a_n^\alpha+\frac{r^{n+1}}{4(n+1)}e_n^\alpha+b_n^\alpha r^{-n}+g_n^\alpha r^n \qquad (n\geq 2), \tag{33}$$

and similar expressions for $\tilde{f}_n^\alpha$. Once again, the coefficients of the singular terms, e.g. b_n^α, can be related to the multipoles induced by tube α (i.e., A_n^α and B_n^α) and the coefficients of regular terms can be related to the derivatives of the regular part of T_s at $\mathbf{x}=\mathbf{x}^\alpha$. The results are given in the appendix.

Inside tube α, the temperature satisfies (5), a formal solution of which is

$$T_t(\mathbf{x})=-\frac{2}{\alpha_c\phi}\left(\frac{r^2}{4}-\frac{r^4}{16}\right)+\sum_{n=0}^{\infty}[d_n^\alpha(r)\cos n\theta+\tilde{d}_n^\alpha(r)\sin n\theta]r^n. \tag{34}$$

The coefficients d_n^α and $\tilde{d}_n^\alpha$ can be eliminated upon application of the conditions of continuity of temperature and flux at the surface of the tube, r=1, leading to relations among the coefficients d_n^α, a_n^α, e_n^α, and g_n^α. These coefficients together with the expressions that relate these coefficients to A_n^α and B_n^α lead to a set of equations that can be solved to determine the entire temperature field.

The condition of continuity of flux integrated over the surface of the tube yields

$$B_0^\alpha=\frac{1}{4}A_0^\alpha-\frac{1}{32}G+\frac{1}{4\phi}-\frac{1}{2}A_2^\alpha. \tag{35}$$

Thus, we see the monopole induced is not an unknown. This is a direct consequence of the fact that the total heat lost by each tube is fixed (cf. (12)). On noting that U_0 is given by (24), we see that the condition (29) is automatically satisfied.

The average temperature of the tube side fluid is given by

$$\langle T_t\rangle=-\frac{5}{24}\frac{1}{\alpha_c\phi}+\langle d_0\rangle=\frac{1}{6\alpha_c\phi}-\frac{\langle a_0\rangle}{4}\left(1-\frac{3\phi}{8}\right)+\langle g_0\rangle, \tag{36}$$

where, in deriving the last equality, use has been made of the continuity of temperature at r=1.

The average temperature of the shell side fluid is determined from integrating T_s given by (26) over the entire unit cell and subtracting from it the integrals over the area occupied by the tubes. The latter are evaluated by using the local expansion near each tube (cf. (30)). The resulting expression is

$$\langle T_s\rangle=-\frac{1}{4(1-\phi)}-\frac{\phi\langle g_0\rangle}{1-\phi}+\frac{\phi}{96}\frac{(27-11\phi)}{1-\phi}\langle a_0\rangle$$
$$+\frac{\phi}{1-\phi}\langle b_2\rangle-\frac{\phi}{24(1-\phi)}\langle a_4\rangle. \tag{37}$$

The difference between the average temperatures of the tube and shell side fluids is given by

$$\Delta T=\langle T_t\rangle-\langle T_s\rangle=\frac{1}{6\alpha_c\phi}+\frac{1}{4(1-\phi)}$$
$$-\frac{\langle a_0\rangle}{4}\frac{12-3\phi-\phi^2}{12(1-\phi)}+\frac{\langle g_0\rangle}{1-\phi}+\frac{\phi}{1-\phi}\langle b_2\rangle-\frac{\phi}{24(1-\phi)}\langle a_4\rangle. \tag{38}$$

It is customary to write the overall heat transfer coefficient in terms of individual heat transfer coefficients on the shell and tube sides. The tube side temperature drop is easily calculated and is given by

$$\Delta T_t=\langle T_t\rangle-\langle T_w\rangle=\frac{1}{6\alpha_c\phi}. \tag{39}$$

The tube side Nusselt number is therefore given by

$$Nu_t=\frac{1}{2\alpha_c\phi\Delta T_t}=3. \tag{40}$$

This is, of course, is the well-known result for the tube side Nusselt number for the Graetz problem based on constant wall heat flux. We now define the shell side Nusselt number Nu_s via

$$\frac{1}{Nu_s}=\frac{1}{Nu_{overall}}-\frac{1}{\alpha_c Nu_t}=2\phi\Delta T_s, \tag{41}$$

where $\Delta T_s=\Delta T-\Delta T_t$ is the shell side temperature difference.

For determining Nusselt numbers based on mixing-cup temperature differences (cf. (10)), we need to integrate the product u_sT_s over the area occupied by the shell side fluid. This is difficult because it would require evaluating S_1, S_2, and their derivatives at many points outside the tubes. It is more efficient instead to solve for an auxiliary function ψ defined by

$$\nabla^2\psi=T_s, \qquad \psi=0 \qquad \text{at } |\mathbf{x}-\mathbf{x}^\alpha|=1. \tag{42}$$

Substituting for T_s from (42) into (10) and using Green's theorem we obtain

$$\tau\langle T_s\rangle_c=\int_{D_s}u_sT_s dA=\int_{D_s}u_s\nabla^2\psi dA$$
$$=\int_{D_s}\psi\nabla^2 u_s dA+\int_{\partial D_s}(u_s\nabla\psi-\psi\nabla u_s)\cdot\mathbf{n}dl. \tag{43}$$

The integral over ∂D_s, which consists of the unit cell boundary and the surface of the tubes, vanishes owing to the boundary condition $u_s=\psi=0$ on the tube surface and the spatial periodicity of ψ and u_s. On using (14) we obtain

$$\langle T_s\rangle_c=\frac{G}{\tau}\int_{D_s}\psi dA. \tag{44}$$

A formal expression for ψ can be written in the same way as for u_s and T_s:

$$\psi(\mathbf{x})=\psi_0+\sum_{\alpha=1}^{N}\sum_{n=0}^{\infty}[C_n^\alpha\partial_1^n+\tilde{C}_n^\alpha\partial_1^{n-1}\partial_2]S_1$$
$$+[B_n^\alpha\partial_1^n+\tilde{B}_n^\alpha\partial_1^{n-1}\partial_2]S_2+[A_n^\alpha\partial_1^n+\tilde{A}_n^\alpha\partial_1^{n-1}\partial_2]S_3 \tag{45}$$

where S_1, S_2 and S_3, and their derivatives, are to be evaluated at $\mathbf{x}-$

$\mathbf{x}^\alpha$, and $\nabla^2 S_3 = S_2$. Expression (28) with m=3 can be used to evaluate S_3. The coefficients ψ_0, C_n and $\tilde{C}_n$ are to be evaluated from the boundary condition $\psi=0$ on the surface of the tubes. Finally, since $\nabla^2 S_1 = 4\pi/\tau$ at all points outside the tubes, we require that

$$\sum_{\alpha=1}^{N} C_0^\alpha = 0. \tag{46}$$

To determine the coefficients $\tilde{C}_n^\alpha$, we expand ψ near the surface of each tube as

$$\psi = \sum_{n=0}^{\infty} \psi_n(r)\cos n\theta + \psi_n(r)\sin n\theta \tag{47}$$

with

$$\psi_n = \psi_n^r + \psi_n^s, \tag{48}$$

$$\psi_n^r = h_n r^n + \frac{g_n}{4(1+n)} r^{n+2} + \frac{e_n}{32(n+1)(n+2)} r^{n+4} + \frac{G}{32\cdot 12\cdot 6} r^6 \delta_{n0} \quad (n \geq 0). \tag{49}$$

For the purpose of applying boundary conditions at r=1, we evaluate ψ_n^s at r=1 using

$$\psi_n^s(1) = \beta_1 A_n + \beta_2 A_{n+2} + \beta_3 A_{n+4} + \beta_4 B_n + \beta_5 B_{n+2} + \beta_6 C_n, \tag{50}$$

where

$$\beta_1 = \frac{(-1)^n (n-3)!}{16}, \qquad \beta_2 = \frac{(-1)^{n+1}(n-2)!(n+2)}{8},$$
$$\beta_3 = \frac{(-1)^n n!(n+3)(n+4)}{16n}, \qquad \beta_4 = \frac{(-1)^{n+1}(n-2)!}{8},$$
$$\beta_5 = \frac{(-1)^{n+1} n!(n+2)}{2n}, \qquad \beta_6 = 2(-1)^n (n-1)!$$
$$\beta_1 = 3/64, \quad \beta_2 = 1/4, \quad \beta_4 = 1/2, \quad \beta_3 = \beta_5 = \beta_6 = 0 \qquad \text{for } n=0,$$
$$\beta_1 = 5/32, \quad \beta_2 = 3/8, \quad \beta_4 = 1/2 \qquad \text{for } n=1,$$
$$\beta_1 = 3/32 \qquad \text{for } n=2. \tag{51}$$

Now the integral of ψ over the area occupied by the shell side fluid can be determined by integrating ψ given by (45) over the unit cell first and then subtracting from it the integrals inside the tubes by using the expression (47) for ψ near each tube. The final result for the mixing-cup based temperature difference is

$$\Delta T_c = \Delta T_{t,c} + \Delta T_{s,c} \tag{52}$$

with

$$\Delta T_{t,c} = \frac{11}{48\phi}, \qquad Nu_{t,c} = \frac{1}{2\phi \Delta T_{t,c}} = \frac{24}{11}, \tag{53}$$

$$\Delta T_{s,c} = \frac{1}{2\phi Nu_{s,c}} = \langle g_0 \rangle + \frac{\langle A_0 \rangle}{2} - \frac{3G}{64} + G\phi\left[\frac{5}{32\cdot 9}\langle A_0 \rangle + \frac{5}{32}\langle A_2 \rangle + \frac{3}{8}\langle A_4 \rangle + \frac{5}{4}\langle A_6 \rangle + \frac{5}{16}\langle B_0 \rangle + \frac{\langle B_2 \rangle}{2} - \frac{3}{2}\langle B_4 \rangle + \langle C_0 \rangle - 2\langle C_2 \rangle + \langle h_0 \rangle + \frac{\langle g_0 \rangle}{8} + \frac{\langle e_0 \rangle}{32\cdot 6} + \frac{G}{32\cdot 12\cdot 8\cdot 6} - \frac{\psi_0}{\phi}\right]. \tag{54}$$

RESULTS AND DISCUSSION

Table 1 shows Nusselt numbers at selected values of ϕ and α_c for square as well as hexagonal arrays of tubes. It is seen that the mixing-cup based Nusselt number is smaller than that based on area average. This is to be expected since the mixing-cup based temperature of the shell side fluid is weighted by the fluid velocity that generally increases with the increase in the radial distance from the tube. The temperature difference, which is inversely related to the Nusselt number, is greater for the mixing-cup based temperature since the difference between the shell side fluid and tube wall temperature increases in magnitude with the increase in the distance from the tube wall. We also see that the Nusselt numbers depend

Table 1. Nu_s and $Nu_{s,c}$ as functions of α_c and ϕ for square and hexagonal arrays

ϕ	α_c	Nu_s Square array	Nu_s Hexagonal array	$Nu_{s,c}$ Square array	$Nu_{s,c}$ Hexagonal array
0.2	0	2.166	2.311	1.856	2.040
	1	2.167	2.311	1.858	2.040
	10	2.167	2.311	1.859	2.040
	∞	2.167	2.311	1.859	2.040
0.4	0	2.469	4.443	2.575	3.760
	1	3.515	4.444	2.626	3.762
	10	3.551	4.445	2.667	3.763
	∞	3.559	4.445	2.675	3.763
0.6	0	3.193	7.584	1.884	5.721
	1	3.795	7.584	2.300	5.853
	10	4.248	7.763	2.627	5.954
	∞	4.344	7.780	2.699	5.976

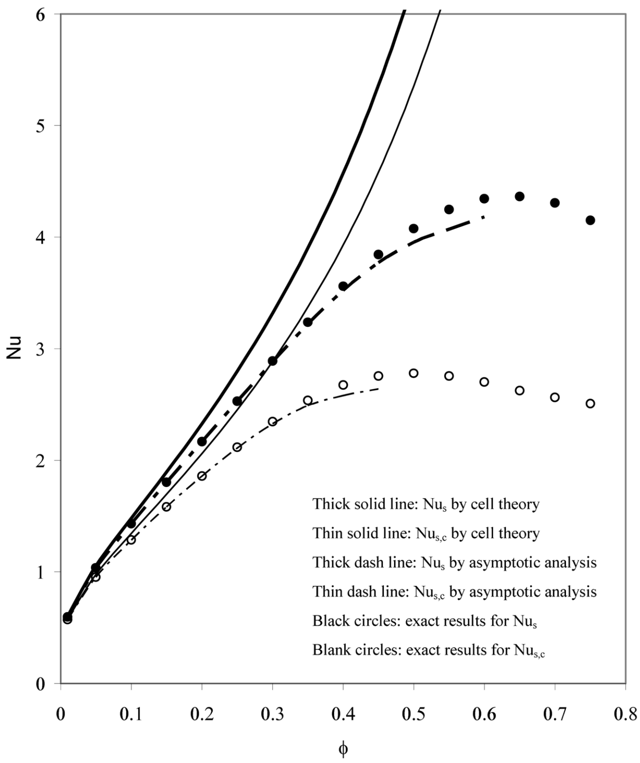

Fig. 2. Nusselt numbers, Nu_s and $Nu_{s,c}$, as functions of ϕ for square array of tubes.

on the ratio of conductivities α_c only slightly at moderate values of ϕ but that the dependence becomes stronger at high values of ϕ. We also note that Nusselt numbers for hexagonal arrays are greater than those for square arrays at the same ϕ. The different Nusselt numbers for two arrays come from the configuration difference. Six neighboring tubes near a tube at origin are placed at equal distance from the tube at origin in hexagonal array while the tube at the origin in the square array is surrounded by four adjacent tubes and another four tubes with larger distance from the tube at the origin. The distance from tube at the origin to the nearest tubes is shorter for the case of square array at the same area fractions of tubes, and thus it is expected that heat transfer rate is much reduced for the region where the distance between the tubes is small.

Figs. 2 and 3 show the numerical results for Nusselt numbers for $\alpha_c=\infty$. Nusselt numbers are seen to increase with the increase in area fraction at small to moderate area fractions. At small ϕ, the heat must diffuse a greater distance into the shell side fluid, and this increases ΔT_s. Interestingly, the Nusselt number seems to go through a maximum at very high ϕ. The solid lines in these figures represent the predictions of an asymptotic analysis and dashed lines show the predictions from the cell theory to be described next.

The analysis for small ϕ is similar to one presented by Hasimoto [1959] and Sangani and Acrivos [1982] who considered the problem of determining drag force on spherical particles. This analysis yields the following results for Nusselt numbers for square and hexagonal arrays:

$$\mathrm{Nu}_s^{-1}=\frac{2\phi}{1-\phi}\left[\mathrm{g}_0+\frac{1}{4}+\frac{\mathrm{A}_0}{2}+\frac{\mathrm{A}_0\beta_c}{4}\phi\mathrm{S}_1^r+\left(\frac{\beta_c}{4}-\frac{\mathrm{A}_0}{8}\right)\phi+\left(\frac{\beta_c}{2}-\frac{1}{24}\right)\phi^2-\left(\frac{\partial_1^4\mathrm{S}_1^r}{2\cdot 2\cdot 3!\cdot 4!}+\frac{\beta_c\mathrm{A}_0}{8}\right)\phi^3\right], \tag{55}$$

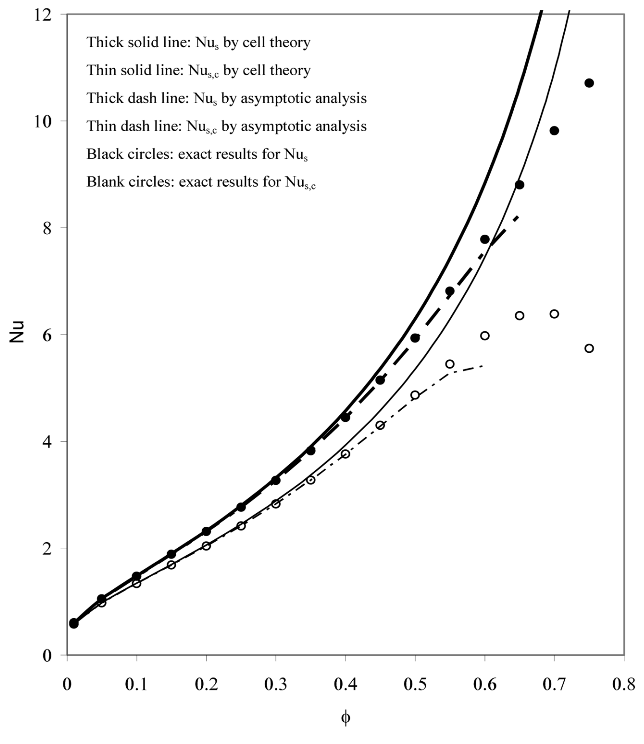

Fig. 3. Nusselt numbers, Nu_s and $\mathrm{Nu}_{s,c}$, as functions of ϕ for hexagonal array of tubes.

Table 2. S_1^r, S_2^r, S_3^r and their derivatives at r=0 as functions of ϕ for square and hexagonal arrays

	n	Square array	Hexagonal array
$\partial_1^n\mathrm{S}_1^r$	0	$-\log\phi-1.4763$	$-\log\phi-1.4975$
	2	2ϕ	2ϕ
	4	$3.83314\phi^2$	0
	6	0	$29.4765\phi^3$
	8	$440.392\phi^4$	0
$\partial_1^n\mathrm{S}_2^r$	0	$-0.1527/\phi$	$-0.1465/\phi$
	4	0.7018ϕ	1.5ϕ
$\partial_1^n\mathrm{S}_3^r$	0	$0.1465\times10^{-3}/\phi^2$	$-8.35\times10^{-4}/\phi^2$

$$\mathrm{Nu}_{s,c}^{-1}=2\phi\left[\mathrm{g}_0+\frac{\mathrm{A}_0}{2}\left(1-\frac{3}{8}\phi\right)-4\phi\mathrm{A}_0\psi_0+4\phi^2\mathrm{A}_0\left\{\mathrm{A}_0\frac{40-11\phi}{32\cdot 72}+\frac{5}{16}\mathrm{B}_0-\frac{\mathrm{A}_0\beta_c}{16}\mathrm{S}_1^r-\frac{\beta_c}{16}-\frac{\beta_c\mathrm{A}_0}{8}\phi+\frac{\mathrm{A}_0}{2}\left(\frac{\partial_1^4\mathrm{S}_1^r}{2\cdot 3!\cdot 4!\phi^2}+\frac{\beta_c}{16}\right)\phi^2+\mathrm{h}_0+\frac{\mathrm{g}_0}{8}\right\}\right], \tag{56}$$

where

$$\mathrm{B}_0=\frac{1}{4\phi}+\frac{\mathrm{A}_0}{4}\left(1-\frac{\phi}{2}\right),\qquad \beta_c=\frac{\alpha_c-1}{\alpha_c+1},$$

$$\mathrm{g}_0=\mathrm{A}_0\mathrm{S}_2^r+\mathrm{B}_0\mathrm{S}_1^r-\mathrm{A}_0\frac{\partial_1^4\mathrm{S}_1^r\partial_1^4\mathrm{S}_2^r}{2\cdot 3!\cdot 4!}-\partial_1^2\mathrm{S}_1^r\left[\frac{\beta_c\mathrm{A}_0}{8}\mathrm{S}_1^r+\frac{\beta_c}{8}+\frac{\beta_c\mathrm{A}_0}{4}\phi-\mathrm{A}_0\left(\frac{\partial_1^4\mathrm{S}_1^r}{2\cdot 3!\cdot 4!\phi}+\frac{\beta_c}{16}\right)\phi^2\right]$$

$$\mathrm{h}_0=-\mathrm{A}_0\frac{27-8\phi}{32\cdot 18}-\frac{\mathrm{B}_0}{2}-\frac{\mathrm{g}_0}{4},$$

$$\psi=\mathrm{h}_0-\mathrm{A}_0\mathrm{S}_3^r-\mathrm{B}_0\mathrm{S}_2^r+\mathrm{S}_1^r\left[\frac{\beta_c\mathrm{A}_0}{16}\mathrm{S}_1^r+\frac{\beta_c}{16}+\frac{\beta_c\mathrm{A}_0}{8}\phi-\frac{\mathrm{A}_0}{2}\left(\frac{\partial_1^4\mathrm{S}_1^r}{2\cdot 3!\cdot 4!\phi^2}+\frac{\beta_c}{16}\right)\phi^2\right]. \tag{57}$$

Here, the superscript r in S_1^r, S_2^r and S_3^r and their derivatives denote the regular part of these functions at r=0. Their values for square and hexagonal arrays are listed in Table 2.

In addition to the asymptotic analysis for small area fractions of tubes, we also compare the results of exact calculations with the predictions obtained using a cell theory [Happel, 1959], which is more appropriate for periodic arrays than effective-medium theory. In this theory, the periodic unit cell is replaced by a fluid cell of outer radius $\mathrm{R}=\phi^{-1/2}$ and inner radius unity. The fluid velocity is given by

$$u_s=-2\mathrm{A}_0\log r+\frac{G}{4}r^2+e_0. \tag{58}$$

The constants are determined by using the boundary conditions $u_s=0$ at r=1 and $\partial u_s/\partial r=0$ at r=R, and the condition that the average velocity of the fluid in the cell equals $1/(1-\phi)$. This yields

$$-\frac{1}{\mathrm{A}_0}=\log\mathrm{R}^2-\frac{3}{2}+\frac{2}{\mathrm{R}^2}-\frac{1}{2\mathrm{R}^4} \tag{59}$$

and $G=4\phi\mathrm{A}_0$.

The temperatures for the shell and tube side fluids are given by

$$T_s=\mathrm{A}_0\left[\frac{1}{2}r^2(1-\log r)+\frac{1}{\mathrm{R}^2}\left(\frac{r^4}{16}-\frac{r^2}{4}\right)\right]-2\mathrm{B}_0\log r+\mathrm{C}_0 \quad \text{for } r>1 \tag{60}$$

$$T_t=-\frac{2}{\alpha_c\phi}\left(\frac{r^2}{4}-\frac{r^4}{16}\right) \quad \text{for } r<1. \tag{61}$$

The constants B_0 and C_0 are determined by using the conditions of continuity of temperature and flux at r=1. The condition of no flux at r=R is automatically satisfied. The average temperatures of the fluids, and hence the Nusselt numbers, can be determined once these two constants are determined. The results for the Nusselt numbers are given below.

$$\frac{1}{\mathrm{Nu}_s}=-2\phi\left[\mathrm{C}_0+\frac{3}{8\alpha_c\phi}+\frac{2}{\mathrm{R}^2-1}\left\{\mathrm{A}_0\left(\frac{\mathrm{R}^4}{6}-\frac{\mathrm{R}^4\log\mathrm{R}}{8}-\frac{\mathrm{R}^2}{16}-\frac{5}{48}\right)\right.\right.$$
$$\left.\left.+\mathrm{B}_0\left(-\mathrm{R}^2\log\mathrm{R}+\frac{\mathrm{R}^2-1}{2}\right)\right\}\right], \tag{62}$$

$$\frac{1}{\mathrm{Nu}_{s,c}}=-2\phi\left[\mathrm{C}_0+\frac{3}{8\alpha_c\phi}+\frac{2}{\mathrm{R}^2}\left\{\mathrm{A}_0^2\left\{\left(-\frac{\mathrm{R}^4\log\mathrm{R}}{4}+\frac{1}{16}(\mathrm{R}^4-1)\right)\left(1-\frac{1}{\mathrm{R}^2}\right)\right.\right.\right.$$
$$+\frac{5}{48}\left[-\mathrm{R}^2\log\mathrm{R}+\frac{1}{6}\left(\mathrm{R}^4-\frac{1}{\mathrm{R}^2}\right)\right]+\frac{\mathrm{R}^4}{8}\log\mathrm{R}(2\log\mathrm{R}-1)$$
$$+\frac{1}{32}(\mathrm{R}^4-1)+\frac{1}{2\mathrm{R}^2}\left(\frac{\mathrm{R}^6}{6}-\frac{\mathrm{R}^4}{4}+\frac{1}{12}\right)+\frac{1}{\mathrm{R}^4}\left(\frac{\mathrm{R}^8}{128}-\frac{5\mathrm{R}^6}{96}\right.$$
$$\left.\left.+\frac{\mathrm{R}^4}{16}-\frac{7}{384}\right)\right\}+\mathrm{A}_0\mathrm{B}_0\left\{2\mathrm{R}^2\left((\log\mathrm{R})^2-\log\mathrm{R}+\frac{1}{2}\right)\right.$$
$$\left.\left.\left.-1-\frac{2}{\mathrm{R}^2}\left(\frac{\mathrm{R}^4}{4}\log\mathrm{R}-\frac{\mathrm{R}^4-1}{16}-\frac{\mathrm{R}^2}{2}\log\mathrm{R}+\frac{\mathrm{R}^2-1}{4}\right)\right\}\right\}\right]. \tag{63}$$

Figs. 2 and 3 compare the predictions of the cell theory with the exact results for Nusselt numbers. The cell theory results are generally in better agreement with those for hexagonal arrays than for square arrays. This agreement results from the observation that hexagonal arrays of tubes are geometrically closer to the cell model than the square arrays are, as shown in Fig. 1. In all cases, however, the results obtained from the low ϕ analysis yield more accurate results than those obtained using the cell theory. Since the asymptotic analysis for low ϕ uses asymptotic expressions for spatially periodic functions S_1^r, S_2^r and S_3^r and their derivatives that directly give velocity and temperature field while the cell theory employs a simple model consisting of a tube and encapsulating cell, it is seen that the asymptotic analysis shows agreement with numerical simulations for wider range of area fractions of tubes than the cell theory does.

CONCLUSION

We determined Nusselt numbers for shell side longitudinal flow along the axes of tubes in square and hexagonal arrays. The shell side Nusselt numbers, which are related to the inverse of average temperature difference between shell side and tube wall, are computed based on two kinds of average temperatures, i.e., spatial average and mixing-cup temperature. Nusselt numbers with mixing-cup temperature are smaller than those based on spatial average temperature, because the difference between the temperatures of shell side and tube wall increases with the distance from the tube wall as does fluid velocity by which mixing-cup temperature is weighted. The shell side Nusselt numbers for hexagonal arrays are larger than those for square arrays, saying hexagonal arrays are more efficient for convective heat transfer on the shell side. The Nusselt numbers of shell side count on the ratio of thermal conductivities of fluids in the tube and shell side. At small area fractions of tubes the dependence on the conductivity ratio is weak but it becomes stronger at high area fractions of tubes.

Numerical results for Nusselt numbers are compared with those by a cell theory. At small area fractions of tubes, the cell theory agrees quite well with the numerical results. At larger area fractions, the cell theory gives better estimates for hexagonal arrays. An asymptotic analysis for small area fractions is also performed and shown to give more accurate results than does the cell theory for both square and hexagonal arrays.

ACKNOWLEDGMENTS

The authors acknowledge Professor Ashok S. Sangani and Syracuse University, NY, U. S. A. for the support of this work. The computations were performed using the resources by the National Center for Supercomputing Applications at University of Illinois at Urbana-Champaign.

APPENDIX

1. Derivatives of Singular Parts of S_1, S_2, and S_3

$$\mathrm{S}_1^s=-2\log\mathrm{r} \tag{A1}$$

$$\partial_1^n\mathrm{S}_1^s=2(-1)^n(\mathrm{n}-1)!\mathrm{r}^{-n}\cos\mathrm{n}\theta \tag{A2}$$

$$\partial_1^{n-1}\partial_2\mathrm{S}_1^s=2(-1)^n(\mathrm{n}-1)!\mathrm{r}^{-n}\sin\mathrm{n}\theta \tag{A3}$$

$$\mathrm{S}_2^s=\frac{1}{2}\mathrm{r}^2(1-\log\mathrm{r}) \tag{A4}$$

$$\partial_1^n\mathrm{S}_2^s=\frac{1}{2}(-1)^{n+1}(\mathrm{n}-2)!\mathrm{r}^{2-n}\left[\cos\mathrm{n}\theta-\frac{\mathrm{n}}{\mathrm{n}-2}\cos(\mathrm{n}-2)\theta\right] \tag{A5}$$

$$\partial_1^{n-1}\partial_2\mathrm{S}_2^s=\frac{1}{2}(-1)^{n+1}(\mathrm{n}-2)!\mathrm{r}^{2-n}\left[\sin\mathrm{n}\theta-\frac{\mathrm{n}}{\mathrm{n}-2}\sin(\mathrm{n}-2)\theta\right] \tag{A6}$$

$$\mathrm{S}_3^s=\frac{1}{64}\mathrm{r}^4(3-2\log\mathrm{r}) \tag{A7}$$

$$\partial_1^n\mathrm{S}_3^s=\frac{1}{32}(-1)^n(\mathrm{n}-4)!\mathrm{r}^{4-n}\left[\frac{2\mathrm{n}(\mathrm{n}-1)}{\mathrm{n}-4}\cos(\mathrm{n}-4)\theta\right.$$
$$\left.-4\mathrm{n}\cos(\mathrm{n}-2)\theta+2(\mathrm{n}-3)\cos\mathrm{n}\theta\right] \tag{A8}$$

$$\partial_1^{n-1}\partial_2\mathrm{S}_3^s=\frac{1}{32}(-1)^n(\mathrm{n}-4)!\mathrm{r}^{4-n}[2\mathrm{n}(\mathrm{n}-1)\sin(\mathrm{n}-4)\theta$$
$$-4\sin(\mathrm{n}-2)\theta+2(\mathrm{n}-3)\sin\mathrm{n}\theta] \tag{A9}$$

2. Formulas for Determining the Coefficients of Regular Terms

$$\mathrm{g}_n^\alpha=\frac{1}{\mathrm{n}!}\partial_1^n\mathrm{T}_s^r(\mathbf{x}^\alpha)-\frac{\mathrm{e}_{n-2}^\alpha}{4(\mathrm{n}-1)}-\frac{\mathrm{G}}{64}\delta_{n4} \tag{A10}$$

$$\tilde{\mathrm{g}}_n^\alpha=\frac{1}{\mathrm{n}!}\partial_1^{n-1}\partial_2\mathrm{T}_s^r(\mathbf{x}^\alpha)-\frac{\tilde{\mathrm{e}}_{n-2}^\alpha}{4(\mathrm{n}-1)}\frac{\mathrm{n}-2}{\mathrm{n}} \tag{A11}$$

$$\mathrm{h}_n^\alpha=\frac{1}{\mathrm{n}!}\partial_1^n\psi^r(\mathbf{x}^\alpha)-\frac{\mathrm{g}_{n-2}^\alpha}{4(\mathrm{n}-1)}-\frac{\mathrm{e}_{n-4}^\alpha}{32(\mathrm{n}-2)(\mathrm{n}-3)}-\frac{\mathrm{G}}{32\cdot12\cdot6}\delta_{n6} \tag{A12}$$

$$\tilde{\mathrm{h}}_n^\alpha=\frac{1}{\mathrm{n}!}\partial_1^{n-1}\partial_2\psi^r(\mathbf{x}^\alpha)-\frac{\mathrm{n}-2}{\mathrm{n}}\frac{\tilde{\mathrm{g}}_{n-2}^\alpha}{4(\mathrm{n}-1)}-\frac{\mathrm{n}-4}{\mathrm{n}}\frac{\tilde{\mathrm{e}}_{n-4}^\alpha}{32(\mathrm{n}-2)(\mathrm{n}-3)} \tag{A13}$$

NOMENCLATURE

a : radius of tubes
c_p : specific heat of the shell side fluid
c_{pt} : specific heat of the tube side fluid
D_s : area occupied by the shell side fluid
G : pressure gradient non-dimensionalized by $\mu U/a^2$ in axial direction of tubes
$h_{overall}$: overall heat transfer coefficient
k : thermal conductivity of the shell fluid
$Nu_{overall}$: overall Nusselt number
Nu_s : shell side Nusselt number
Nu_t : tube side Nusselt number
Pe : Peclet number
r : radial distance from the center of the tube at origin
Q : rate of heat transfer per tube per unit length of the exchanger
T_s : temperature of shell side fluid
T_t : temperature of tube side fluid
$<T_s>$: spatial average temperature of shell side fluid
$\Delta T_{overall}$: difference between the average temperatures of the fluid on the tube and shell side
U : superficial velocity of the fluid on the shell side
u_s : velocity of the shell-side fluid non-dimensionalized by U
u_t : velocity of the tube-side fluid non-dimensionalized by U
$\mathbf{x}^\alpha$: position vector of the center of tube α
$\mathbf{x}_L$: coordinates (position vector) of the lattice points of the array
α_c : ratio of thermal conductivity of tube-side fluid to that of shell-side fluid
δ : Dirac's delta function
ϕ : area fraction of the tubes
ρ : density of the shell fluid
ρ_t : density of the tube side fluid
τ : unit cell area non-dimensionalized by a^2
μ : viscosity of fluid

REFERENCES

Acrivos, A., "The Extended Graetz Problem at Low Peclet Numbers," *Appl. Sci. Res.*, **36**, 35 (1980).

Bird, R. B., Stewart, W. B. and Lightfoot, E. N., *Transport Phenomena*, 1st ed., Wiley, New York (1960).

Happel, J., "Viscous Flow Relative to Arrays of Cylinders," *AIChE J.*, **5**, 174 (1959).

Hasimoto, H., "On the Periodic Fundamental Solutions of the Stokes Equations and Their Application to Viscous Flow Past a Cubic Array of Spheres," *J. Fluid Mech.*, **5**, 317 (1959).

Kim, W.-K. and Aicher, T., "Experimental Investigation of Heat Transfer in Shell-and-tube Heat Exchangers Without Baffles," *Korean J. Chem. Eng.*, **14**, 93 (1997).

Koo, S. and Sangani, A. S., "Mass Transfer Coefficients for Laminar Longitudinal Flow in Hollow-fibre Contactors," *J. Fluid Mech.*, **484**, 255 (2003).

Papoutsakis, E. and Ramkrishna, D., "Conjugated Graetz Problems. I. General Formalism and a Class of Solid-fluid Problems," *Chem. Eng. Sci.*, **36**, 1381 (1981).

Sangani, A. S. and Acrivos, A., "Slow Flow through a Periodic Array of Spheres," *Int. J. Multiphase Flow*, **8**, 343 (1982).

Sangani, A. S. and Yao, C., "Transport Processes in Random Arrays of Cylinders. II. Viscous Flow," *Phys. Fluids*, **31**, 2435 (1988).

Sparrow, E. M., Loeffler, A. L. and Hubbard, H. A., "Heat Transfer to Longitudinal Laminar Flow Between Cylinders," *J. Heat Transfer*, **83**, 415 (1961).

Wang, W. and Sangani, A. S., "Nusselt Number for Flow Perpendicular to Arrays of Cylinders in the Limit of Small Reynolds and Large Peclet Numbers," *Phys. Fluids*, **9**, 1529 (1997).